

RAPID COMMUNICATION

***Arthrinium sacchari* – a novel causal agent of ripe rot on grapevine (*Vitis vinifera*)**

Zahra Vesaltalab¹, Mansour Gholami¹, Jalal Soltani^{2*} ¹Department of Horticulture, Agriculture Faculty, Bu-Ali Sina University, Hamedan, Iran²Phytopathology Section, Plant Protection Department, Bu-Ali Sina University, Hamedan, Iran

Vol. 66, No. 1: 128–130, 2026

DOI: 10.24425/jppr.2026.158063

Received: October 14, 2025

Accepted: November 25, 2025

Online publication: February 06, 2026

*Corresponding address:

Soltani@basu.ac.ir

Responsible Editor:

Sebastian Stenglein

Abstract

During a survey conducted in Hamedan Province, Iran, Thompson seedless grapevine (*Vitis vinifera*) bunches were observed exhibiting symptoms of brown ripe rot. To identify the causal agent, samples were collected, and fragments from the infected tissues were cultured on PCA and PDA media. Morphological studies and sequencing analyses of the ITS region were performed to identify the emerging fungus. To confirm the pathogenicity of the fungal isolate, Koch's postulates were applied. Based on morphological assessments, pathogenicity test, and the ITS sequences, the causal agent was identified as *Arthrinium sacchari* (Apiosporaceae, Sordariomycetes). This study provides new information on ripe rot caused by *A. sacchari* in grapevine plants.

Keywords: ITS, pathogenicity, Sordariomycetes, taxonomy, *Vitis vinifera*

Grapevine (*Vitis vinifera* L.) is an important horticultural crop worldwide and in Iran (Topfer and Trapp 2022). In 2023, the total harvested area of grapes globally was approximately 6,595,680 hectares, with 113,550 hectares in Iran. Global production was 72,486,522.15 tonnes, with 1,473,241.99 tonnes in Iran (FAO 2023). However, grapevines are susceptible to various fungal pathogens, including *Alternaria alternata*, *Aspergillus carbonarius*, *Botrytis cinerea*, *Cladosporium herbarum*, *Elsinoë ampelina*, *Eutypa lata*,

Guignardia bidwellii, *Mucor racemosus*, *Plasmopara viticola*, *Penicillium expansum*, *Phomopsis viticola*, *Rhizopus nigricans* and *Uncinula necator* (Wilcox et al. 2015). During a survey conducted in Hamedan Province, Iran, Thompson seedless grapevine bunches were observed with symptoms of brown ripe rot lesions, with emerged fungal mycelia, in August at the time of ripening (Fig. 1A). The initial appearance of the symptoms, as well as the white and gray hyphal coating, was very similar to those of *Botrytis* infections, except that

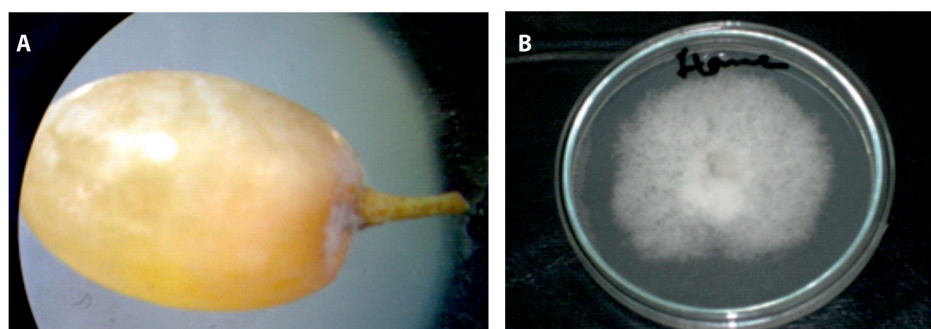


Fig. 1. A – symptoms of brown lesions on grapevine berry; B – *Arthrinium sacchari* colony on PDA after 7 days

the severity of the disease was less than that of gray mold (Jayawardena *et al.* 2018). The lesions were found only on Thompson seedless grapes on very few berries. Although infection was observed in different parts of the berries, the extent of spread on the surface of the berries was also limited. Therefore, no economic damage by this fungus was observed in the monitored vineyards. To identify the causal agent, five tissue samples of approximately 5 × 5 mm were collected from the infected areas. The samples were surface sterilised by immersion in sodium hypochlorite (1% v/v aq) for 1 min, followed by three rinses with sterilised distilled water and drying on sterilised tissue paper. Fragments taken from the border between healthy and infected tissues were then cultured on Potato Carrot Agar (PCA). Fungal hyphae emerging from the fragments were transferred to Potato Dextrose Agar (PDA) to purify the cultures. Mycelial growth rates were measured on PDA after 4 and 7 days in five replicates. For morphological analyses, fungal colonies were grown on PDA at 24°C for 7 days. The fungal species were identified according to the classification system of Ellis (1971). Fungal morphology was characterised using a light microscope (Leitz Diaplan, Germany), and images were captured with a Mercury VQ3240 digital camera (China). Fungal colony images were also taken with a digital camera (Canon PowerShot S410, Japan). The

fungal colony initially appeared floccose and whitish, later turning dark blackish-brown, with a more or less compact structure. It exhibited slow growth, reaching a diameter of 25 mm in 4 days and 60 mm in 7 days at 24°C on PDA (Fig. 1B). The mycelia were partly superficial and partly immersed, with sporulation mainly localised in dark spots within the aerial mycelium. The conidiophores (approximately 1.5 µm) were basauxic, ampulliform, barrel-shaped, or broadly clavate. The conidiophore mother cells were simple, often narrow, cylindrical, and usually colourless. The conidiogenous cells were integrated, terminal and intercalary, polyblastic, denticulate, with short, cylindrical, truncate pegs. The conidia were solitary, lateral, and sometimes terminal, flattened with a hyaline rim, brown, smooth, aseptate, almost round (7.58 µm × 7.70 µm) in surface view, and lenticular in side view, with a germ slit visible at the senescence stage (Fig. 2). Based on these characteristics, the fungus was identified as *Arthrinium sacchari* according to the description by Ellis (1971).

To extract DNA from mycelium, Malt Extract Broth (MEB) was inoculated and incubated at 24°C for 5 days on a rotary shaker (120 rpm). The mycelium was collected on a sterile filter, washed with sterile distilled water, and frozen at -20°C. DNA was extracted according to Murray and Thompson (1980). The ITS1, 5.8S, and ITS2 regions were amplified using primers

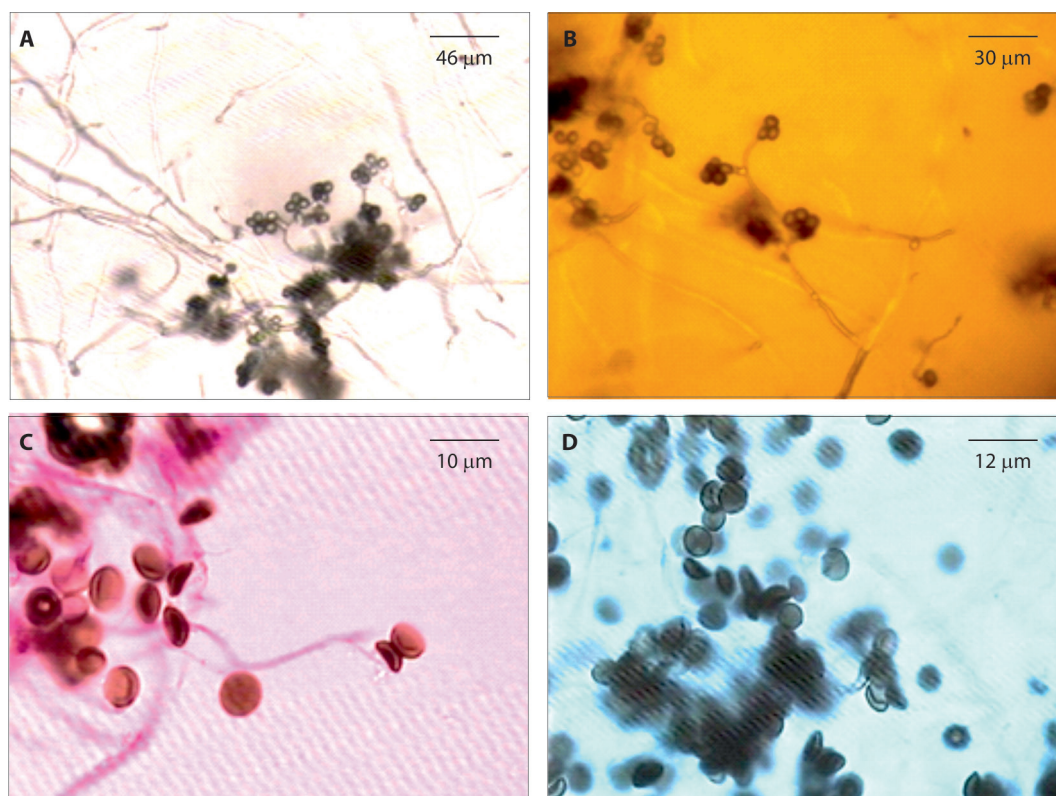


Fig. 2. A and B – different conidiophores and young conidia of *Arthrinium sacchari* from grapes; C and D – lenticular, dark brown conidia with a germ slit

Table 1. List of isolates and ITS sequences used in phylogenetic study with GenBank accession numbers

Species	GeneBank acc. no	Isolate	Host	Location
<i>Apiospora arundis</i>	PV835211.1	CF-166146	<i>Elegia capensis</i> (Cederberg)	South Africa
<i>Apiospora arundis</i>	PQ219333.1	C18	Tobacco leaf	China
<i>Apiospora endophytica</i>	OQ587997.1	ZHKUCC 23-0007	<i>Wurfbainia villosa</i>	China
<i>Apiospora endophytica</i>	OQ587996.1	ZHKUCC 23-0006	<i>Wurfbainia villosa</i>	China
<i>Apiospora malaysiana</i>	MG751214.1	35F5R-AM	<i>Hevea brasiliensis</i> roots	Brazil
<i>Apiospora malaysiana</i>	MF326433.1	SC1	Malaysian seaweed	Malaysia
<i>Apiospora marii</i>	MH873913.1	CBS:497.90	ND*	Spain
<i>Apiospora montagnei</i>	AY787685.2	Olrim927	<i>Fraxinus excelsior</i>	Lithuania
<i>Apiospora neochinense</i>	NR_172409.1	CFCC 53036	ND	China
<i>Apiospora sacchari</i>	OP510133.1	G3	ND	USA
<i>Apiospora sacchari</i>	HQ914941.1	OUCMBI101116	Marine macroalgae	China
<i>Apiospora sacchari</i>	KX778672.1	CNUZ-L53	Fishscale bamboo	China
<i>Apiospora sacchari</i>	HQ914941.1	OUCMBI101116	Marine macroalgae	China
<i>Apiospora vietnamensis</i>	PV490963.1	GUCC 223072	Bamboo	China
<i>Apiospora vietnamensis</i>	PV490962.1	GUCC 223071	Bamboo	China
<i>Arthrinium acutiapicum</i>	MT946342.1	KUMCC 20-0209	Bamboo	China
<i>Arthrinium arundinis</i>	GU566268.1	G41	<i>Phalaris arundinacea</i>	Czech Republic
<i>Arthrinium aureum</i>	AB220246.1	IMI 252326d	ND	Japan
<i>Arthrinium aureum</i>	AB220247.1	IMI 326871	ND	Japan
<i>Arthrinium aureum</i>	AB220251.1	CBS 244.83	ND	Japan
<i>Arthrinium euphorbiae</i>	AB220241.1	IMI 285638b	ND	Japan
<i>Arthrinium euphorbiae</i>	OM728647.1	ZHKU 22-0001	Bamboo dead culms	China
<i>Arthrinium marii</i>	KT023008.1	8	Apple	China
<i>Arthrinium marinum</i>	MH498534.2	KUC21356	Seaweed	South Korea
<i>Arthrinium marinum</i>	ON228604.1	<i>SICAUCC22-0046</i>	ND	ND
<i>Arthrinium phaeospermum</i>	PV368304.1	ZMD16	Bamboo	China
<i>Arthrinium phaeospermum</i>	PV368303.1	ZMD13	Bamboo	China
<i>Arthrinium phaeospermum</i>	PP857519.1	68FN31	ND	China
<i>Arthrinium phaeospermum</i>	OR543752.1	ICMP 6966	Bamboo	New Zealand
<i>Arthrinium phaeospermum</i>	HM222956.1	A229	<i>Taxus chinensis</i> var. <i>mairei</i>	China
<i>Arthrinium phaeospermum</i>	JN198505.1	C29	<i>Taxus chinensis</i> var. <i>mairei</i>	China
<i>Arthrinium phaeospermum</i>	JQ936303.1	CAP35F	Soybean	ND
<i>Arthrinium phaeospermum</i>	JX914483.1	11 LA1-4	<i>Fortunearia sinensis</i>	China
<i>Arthrinium sacchari</i>	JQ269339	IRAN 2025C	Grapevine	Iran
<i>Arthrinium sacchari</i>	HQ115662.1	L06	Indoor air in agricultural soil	Austria
<i>Arthrinium sacchari</i>	HQ115646.1	A09	Indoor air in agricultural soil	Austria
<i>Arthrinium sacchari</i>	KC282388.1	JX1227	<i>Fallopia japonica</i> leaves	China
<i>Arthrinium sacchari</i>	AB693901.1	F0815	Apple leaf	Japan
<i>Arthrinium sacchari</i>	JN628182.1	Z137	Evergreen broad-leaved forest	China
<i>Arthrinium saccharicola</i>	AB220238.1	ATCC 76288	ND	Japan
<i>Arthrinium sargassi</i>	MF615227.2	KUC21287	Marine habitats	South Korea
<i>Arthrinium sargassi</i>	KT207750.1	KUC21232	<i>Sargassum</i> sp.	South Korea
<i>Arthrinium serenense</i>	AB220244.1	IMI 326870	ND	Japan
<i>Arthrinium serenense</i>	AB220250.1	IMI 326869	ND	Japan
<i>Arthrinium serenense</i>	AB220240.1	ATCC 76309	ND	Japan
<i>Arthrinium</i> sp.	MN944538.1	blx-2-65	<i>Thymus mongolicus</i>	China
<i>Arthrinium</i> sp.	LC719237.1	AB-9-2	Artemisia	Japan
<i>Arthrinium</i> sp.	PQ219335.1	C21	Tobacco leaf	China
<i>Nigrospora gorlenkoana</i>	KX986048	CBS 480.73	<i>Vitis vinifera</i>	Kazakhstan

*ND – not determined

The isolate in this study is shown in bold

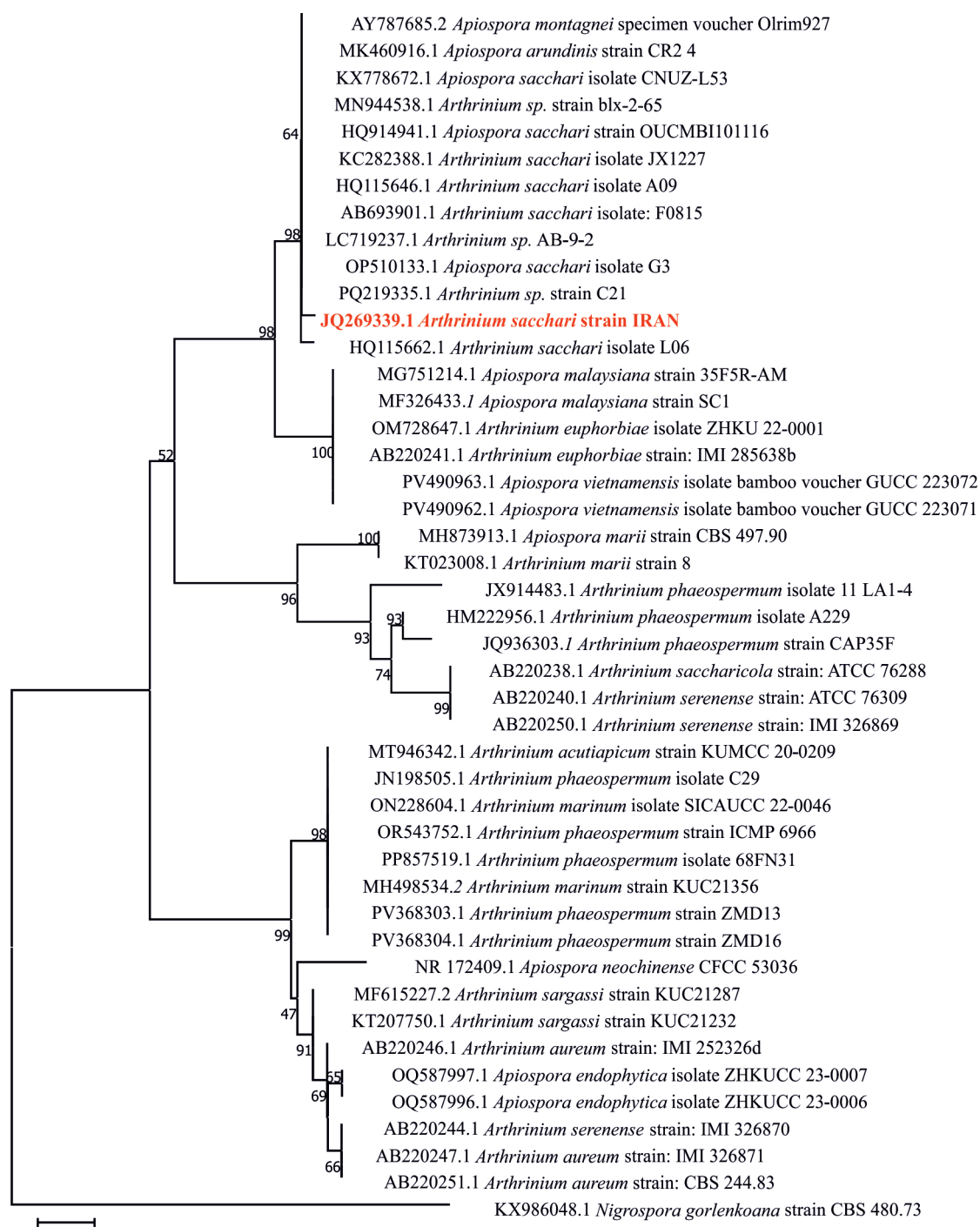


Fig. 3. Phylogenetic tree of the 46 *Arthrinium* isolates inferred by the neighbour-joining method based on ITS sequences. The percentage of replicate trees in which the associated taxa clustered together in the bootstrap test (1000 replicates) is shown next to the branches. The tree is drawn to scale, with branch lengths in the same units as the evolutionary distances used to infer the phylogenetic tree. Complementary information on *Arthrinium* isolates are provided in Table 2

ITS1 and ITS4 (White *et al.* 1990). The PCR was performed in a 25 μ l reaction mixture containing 2.5 μ l of 50 ng \cdot μ l⁻¹ DNA, 12.5 μ l Master Mix (Cinnagen Co., Iran), 2.5 μ l of 10 pmol \cdot μ l⁻¹ of each primer, and 5 μ l H₂O. Amplification was carried out in a TC-512 thermocycler (Techne, UK) under the following conditions: initial denaturation at 96°C for 5 min; 35 cycles of 45 s at 94°C, 30 s at 53°C, and 90 s at 72°C; followed by a final extension at 72°C for 5 min. The amplicon

was sequenced (Macrogen Institute, South Korea). BLASTN was used to query the GenBank database for similarity to *Arthrinium* sequences (approximately 940 bp). Alignments to *Arthrinium* sequences were performed with Clustal W, and a tree was constructed according to Tamura and Nei (1993). Consensus neighbour-joining trees were generated after 1000 bootstrap replicates using MEGA 7.0 (Kumar *et al.* 2016). The representative ITS region sequence was deposited in

GenBank (Accession no. JQ269339). It showed 99% identity with *Arthrimum sacchari* HQ115646 in NCBI. The isolate was deposited in the Iran collection under number IRAN 2025C. An alignment of 46 *Arthrimum* sequences was performed (Table 1) and *Nigrospora gorlenkoana* was used as the out-group taxon. A total of 407 sequence characters were compared. The neighbour-joining tree analysis of the ITS region produced a phylogenetic tree delimiting four main clades with several subgroupings (Fig. 3). All isolates of *A. sacchari* were placed in the first clade. Isolate IRAN 2025C was also found in this clade.

To assess the pathogenicity of the isolate IRAN 2025C on grapes, a suspension of 1.0×10^5 spores \cdot ml⁻¹ was sprayed onto healthy berries that were cut from the rachis with pedicels intact. Sterile distilled water was used as a control. Each group consisted of 30 berries with four replicates per treatment, and the berries were kept at 15°C in darkness for 7 days. The disease severity of each grape was rated on the following scale:

- 0 (healthy berry),
- 1 (one lesion less than 3 mm in diameter),
- 2 (one lesion less than 10 mm in diameter),
- 3 (several lesions or 25% of berry surface infected),
- 4 (more than 26% of the berry surface infected and presence of sporulation).

The disease index (DI) was calculated using the formula (Meng *et al.* 2008)

$$DI = \Sigma(df)/ND$$

d = the severity score

f = the quantity

N = the total number of berries

D = the highest severity level on the scale

The experiment was repeated twice. Infections of the fruits were observed. Spots were observed in various sizes (Table 2) and in different areas of the berries surface. The size of the lesions increased with time. As can be seen in Fig. 2, fungal sporulation was observed on some berries after a storage period of

7 days. Re-isolation of the fungus from inoculated fruits was performed (Fig. 4). The average disease severity on single inoculated berries was calculated to be 0.21875, while in the control group it was 0.08125 (Table 2). With the emergence of the fungus even in control berries, it appears that this pathogen was present in the original vineyards, including in healthy bunches. The decrease in water content of the berries after harvest, the reduction in the resistance of their natural protective barriers, and the increase in relative humidity around the berries due to storage in sterile, sealed containers may explain the growth of the fungus on the control berries. Continued storage of the berries increased fungal sporulation and expansion of infected areas. Symptoms of ripe rot and water loss from the berries also intensified, but no dry berries were observed.

Arthrimum species are primarily saprophytes, plant pathogens, and very often occur as endophytes in a number of plant species. *A. sacchari* has been found on various plants, including *Ananas*, *Borassus*, *Musa*, *Ipomoea*, and *Polygonum* (Ellis 1971), wheat (Mavragani *et al.* 2007), guava (*Psidium guajava* L.)



Fig. 4. Pathogenicity test of *Arthrimum sacchari* on grapevine berry showing lesion and fungal emergence (after 7 days) by artificial inoculation with fungal spore suspension (1.0×10^5 spores \cdot ml⁻¹)

Table 2. Disease severity on inoculated berries with *A. sacchari* spores after 7 days at 15°C

Treatment	Mean of decay index	Replicate	Scale				
			0	1	2	3	4
Control berries	0.08125	1	24	4	2	0	0
		2	24	1	2	1	2
		3	25	2	3	0	0
		4	23	7	0	0	0
Inoculated berries	0.21875	1	20	4	4	2	0
		2	15	8	4	1	2
		3	7	14	7	2	0
		4	13	10	5	2	0

(Elkhateeb 2005), common reed (*Phragmites australis*) (Crous and Groenewald 2013), Carex (Pintos *et al.* 2019), bamboo, sugarcane, swamp grasses, sedges, as well as on lichens (He and Zhang 2012) and marine algae (Suryanarayanan 2012). Moreover, a fungal isolate initially identified as *A. sacchari* was discovered as an endophytic fungus in grapevines in Iran (Hergholi *et al.* 2015). However, the KP749194 accession number for this fungus in NCBI was subsequently updated to *Dothideomyces* sp. To the best of our knowledge, this is the first report of *A. sacchari* in Iran and the first report of its disease-causing ability in grapes.

References

- Crous P.W., Groenewald J.Z. 2013. A phylogenetic re-evaluation of *Arthrinium*. *International Mycological Association Fungus* 4 (1): 133–154.
- Elkhateeb W.A. 2005. Some mycological, phytopathological and physiological studies on mycobiota of selected newly reclaimed soils in Assiut Governorate, Egypt. M.Sc. Thesis, Faculty of Science, Assiut University, Egypt, 238 pp.
- Ellis M.B. 1971. *Dematiaceous Hyphomycetes*. Mycological Institute, CAB, UK.
- FAO. 2023. www.FAO.org [Online] [Sep. 2025].
- He Y., Zhang Z. 2012. Diversity of organism in the *Usnea longissima* lichen. *African Journal of Microbiology Research* 6: 4797–4804.
- Hergholi N., Ghosta Y., Javan-Nikkhah M., Campisano A., Pancher M. 2015. New species of endophytic fungi from grapevine (*Vitis vinifera*) in Iran. *Rostaniha* 16 (1): 17–35.
- Jayawardena R.S., Zhang W., Li X.H., Liu M., Hao Y.Y., Zhao W.S., Hyde K.D., Liu J.H., Yan J.Y. 2018. Characterization of *Botrytis cinerea* causing grape bunch rot in Chinese Vineyards. *Asian Journal of Mycology* 1 (1): 74–87. DOI: 10.5943/ajom/1/1/6
- Kumar S., Stecher G., Tamura K. 2016. MEGA7: molecular evolutionary genetics analysis version 7.0 for bigger datasets. *Molecular Biology and Evolution* 33 (7): 1870–1874. DOI: 10.1093/molbev/msw054
- Mavragani D., Abdellatif L., Conkey B.G., Hamel C., Vujanovic V. 2007. First Report of Damping-Off of Durum Wheat Caused by *Arthrinium sacchari* in the Semi-Arid Saskatchewan Fields. *Plant Disease* 91 (4): 469. DOI: 10.1094/PDIS-91-4-0469A
- Meng X., Li B., Liu J., Tian S. 2008. Physiological responses and quality attributes of table grape fruit to chitosan pre-harvest spray and postharvest coating during storage. *Food Chemistry* 106: 501–508. DOI: doi.org/10.1016/j.foodchem.2007.06.012
- Murray G.C., Thompson W.F. 1980. Rapid isolation of high molecular weight DNA. *Nucleic Acid Research* 8: 4321–4325.
- Pintos A., Alvarado P., Planas J., Jarling R. 2019. Six new species of *Arthrinium* from Europe and notes about *A. caricicola* and other species found in *Carex* spp. *Hosts. MycoKeys* 49: 15–48. DOI: <https://doi.org/10.3897/mycokeys.49.32115>
- Suryanarayanan T.S. 2012. Fungal endosymbionts of seaweeds. p. 53–70. In: “Biology of Marine Fungi” (Raghukumar C., ed.). Springer Dordrecht. DOI: 10.1007/978-3-642-23342-5_3
- Tamura K., Nei M. 1993. Estimation of the number of nucleotide substitutions in the control region of mitochondrial DNA in humans and chimpanzees. *Molecular Biology and Evolution* 33: 1870–1874.
- Topfer R., Trapp O.A. 2022. A cool climate perspective on grapevine breeding: climate change and sustainability are driving forces for changing varieties in a traditional market. *Theoretical and Applied Genetics* 135: 3947–3960. DOI: 10.1007/s00122-022-04077-0
- White T.J., Bruns T., Lee S., Taylor J. 1990. Amplification and direct sequencing of fungal ribosomal RNA genes for phylogenetics. In: “PCR Protocols: a Guide to Methods and Applications” (Innis M.A., Gelfand D.H., Sninsky J.J., White T.J., eds.). Academic Press, San Diego, USA.
- Wilcox W.F., Gubler W.D., Uyemoto J.K. 2015. *Compendium of Grape Diseases, Disorders, and Pests*. 2nd ed. Amer Phytopathological Society, St. Paul, Minnesota.